ELSEVIER

Soil & Tillage Research 64 (2002) 61–78

Soil & Tillage Research

www.elsevier.com/locate/still

Modeling the dynamics of the soil pore-size distribution

Feike J. Leij[a,b,*], Teamrat A. Ghezzehei[c,1], Dani Or[c,2]

[a]USDA-ARS, George E. Brown Jr. Salinity Laboratory, 450 Big Springs Road, Riverside, CA 92507-4617, USA
[b]Department of Environmental Sciences, University of California, Riverside, CA 92502, USA
[c]Department of Plants, Soils, and Biometeorology, Utah State University, Logan, UT 84322, USA

Abstract

Soil tillage often results in a structurally unstable soil layer with an elevated inter-aggregate porosity that is gradually decreased by the interplay of capillary and rheological processes. We have previously proposed to describe the evolution of the pore-size distribution (PSD) with the Fokker–Planck equation (FPE). The coefficients of this equation quantify the drift, dispersion, and degradation processes acting upon the PSD. An analytical solution for the PSD is presented for the case where drift and degradation coefficients depend on time, and the dispersion coefficient is proportional to the drift coefficient. These coefficients can be estimated from independent measurements of the PSD or (surrogate) water retention data or from mechanistic models. In this paper, we illustrate the application of the pore-size evolution model for: (i) a generic drift coefficient, (ii) static water retention data for soils under different tillage regimes, and (iii) dynamic hydraulic data for a soil subject to a sequence of wetting and drying cycles. These applications show the viability of our approach to model pore-size evolution. However, the development and application of the model is hampered by a lack of definitive data on soil structural and hydraulic dynamics.

Keywords: Soil hydraulic properties; Compaction; Wetting; Drying; Pore-size distribution; Analytical solution

1. Introduction

Agronomic management of soils is aimed at providing an optimal habitat for crop production. Soil tillage is used to improve soil structural properties and modifying the soil pore-size distribution (PSD) to create desirable characteristics for gas, water, chemical, and heat movement to facilitate crop growth with minimal environmental degradation due to erosion and groundwater contamination. Because the soil structure after tillage is relatively unstable, the PSD will change with time as a result of wetting and drying, solution composition, agricultural operations, and biological activity. Consequently, associated soil hydraulic and transport properties will also vary over time. Elucidating and quantifying the dynamics of the PSD due to tillage, compaction and other processes will be a difficult undertaking due to the complexity of the pore space and our incomplete understanding of relevant processes. However, there may be considerable payoffs, such as more realistic modeling of subsurface flow and transport or the development of tools to quantify the elusive concept of soil quality.

For aggregated soils, a distinction can be made between textural and structural pore space (Nimmo,

* Corresponding author. Present address: USDA-ARS, George E. Brown Jr. Salinity Laboratory, 450 Big Springs Road, Riverside, CA 92507-4617, USA. Tel.: +1-909-369-4851; fax: +1-909-342-4964.
E-mail addresses: fleij@ussl.ars.usda.gov (F.J. Leij), teamrat@mendel.usu.edu (T.A. Ghezzehei), dani@mendel.usu.edu (D. Or).
[1] Tel.: +1-435-797-2175; fax: +1-435-797-2117.
[2] Tel.: +1-435-797-2637; fax: +1-435-797-2117.

0167-1987/02/$ – see front matter
PII: S0167-1987(01)00257-4

1997). Textural or intra-aggregate pore space, which is determined by the distribution of soil primary particles (i.e., sand, silt and clay), is relatively stable. On the other hand, structural or inter-aggregate pore space, which is determined by the position, orientation, and shape of aggregates relative to one another, tends to be less stable. Inter-aggregate pores approximately correspond to the pores that drain in the water retention range between soil matric potentials 0 and 33 kPa (Ahuja et al., 1984). The latter is approximately equivalent to a pressure head of 330 cm of water (i.e., 330 hPa). These larger pores are most affected by tillage and are also most relevant for managing the capacity of a soil to hold and transmit water and dissolved substances (Gupta and Larson, 1982; Ahuja et al., 1984). Consequently, we are mainly concerned with post-tillage changes associated with structural or inter-aggregate pore space.

Or et al. (2000) proposed to use the Fokker–Planck equation (FPE) to describe the changes in soil pores as a function of time and pore radius and to apply process-based models to estimate the coefficients. The FPE is frequently used to quantify natural processes where the underlying mechanisms cannot be precisely determined (Risken, 1989). Knowledge of the PSD allows prediction of unsaturated soil hydraulic properties with a variety of models such as those by Mualem (1976) and Kosugi (1996). The coefficients of the FPE encompass our understanding of the mathematical behavior of the PSD in response to physical processes. Pore geometry is influenced by mechanical compaction and wetting because of soil settlement, and filling of intra-aggregate pore space. As a result, the porosity and the median pore-size will decrease.

Few, if any, comprehensive data sets exist to calibrate and independently test a model for changes in the PSD. The correctness of the model and our approach can hence not be established. The current paper aims to provide a quantitative framework to soil tillage researchers and others for the evolution of the PSD and to stimulate interest to pursue experimental and theoretical investigations of PSD dynamics. To this end, we will present our model for the PSD and we will illustrate its applicability for scenarios involving soil tillage and irrigation where documented changes in hydraulic properties can be used to infer similar changes in the PSD.

The objectives of the current work are to: (i) describe the model for pore-size evolution and present an analytical solution for the PSD, and (ii) illustrate the model for examples involving a hypothetical case of pore-size evolution, retention data for a particular tillage treatment, and hydraulic data for a series of wetting and drying cycles.

2. Mathematical model

The PSD can be described with the following general partial differential equation, referred to as the FPE (Or et al., 2000):

$$\frac{\partial f}{\partial t} = \frac{\partial}{\partial r}\left(D(r,t)\frac{\partial f}{\partial r}\right) - \frac{\partial}{\partial r}(V(r,t)f) - M(t)f \qquad (1)$$

where f is the PSD or "frequency" (μm^{-1}) as a function of time t (s), and pore radius r (μm), V the drift coefficient ($\mu m\ s^{-1}$), D a dispersion coefficient ($\mu m^2\ s^{-1}$), and M a degradation coefficient (s^{-1}). The drift and dispersion coefficients quantify changes with time of the mean pore radius and the variance of the PSD, respectively. The degradation coefficient represents the fraction of pores that is lost due to instantaneous collapse.

The mathematical conditions are:

$$f(r,0) = f_0(r), \quad 0 < r < \infty \qquad (2)$$

$$Vf - D\frac{\partial f}{\partial r} = 0, \quad r = 0, \ t > 0 \qquad (3)$$

$$\frac{\partial f}{\partial r} = 0, \quad r \to \infty, \ t > 0 \qquad (4)$$

with f_0 as the initial PSD. A plausible choice for the initial distribution is the PSD determined immediately after a tillage event to simulate the PSD until the next event occurs that drastically changes the PSD (e.g., secondary tillage, compaction, etc.). At that time one may continue the simulation by posing a new mathematical problem using a more recent initial condition or one may try to describe the drastic change with a zero-order sink/source term in the original governing equation.

The lower boundary condition (3) stipulates a zero probability flux, i.e., pores cannot assume a negative radius. To ensure conservation, the upper boundary condition requires a zero gradient (which is equivalent

to a zero probability flux for infinitely large pores). The homogeneous zero-flux conditions imply that any loss of probability (PSD) is due to degradation. For the parameterization of the initial distribution, we will use the lognormal distribution according to Kosugi (1994)

$$f_0(r) = \frac{\phi_0}{r\sigma\sqrt{2\pi}} \exp\left(-\frac{[\ln(r/r_0)]^2}{2\sigma^2}\right)$$
$$\text{with} \quad \int_0^\infty f_0(r)\,\mathrm{d}r \equiv \phi_0, \quad 0 < r < \infty \tag{5}$$

where r_0 is the initial median pore radius or geometric mean (μm), σ the standard deviation of the log-transformed pore radius, while ϕ_0 the total (initial) porosity that determines the maximum of the cumulative distribution as defined by Eq. (5). We will assume that ϕ_0 is equal to the difference between saturated and residual water contents $\theta_s - \theta_r$. In aggregated soils consisting of a distinctly bimodal pore space (textural and structural), the total PSD is expressed as a weighted sum of textural and structural distributions (Nimmo, 1997). Further partitioning of the pore space is possible when simulating the PSD (Durner, 1994). The total pore space can be obtained by adding solutions of (1) for each fraction, provided that the superposition principle can be applied.

The physical processes governing the evolution of the PSD are embedded in the coefficients of (1). In the following, we will only consider the case where these coefficients depend on time in a mathematical sense. In reality, pore-size evolution will be determined by factors that affect the energy status of soil aggregates such as rainfall, pore-size, and soil moisture status. The drift coefficient can be estimated from the change in the mean pore radius or the first-order normalized moment of the PSD with respect to the time interval. The degradation coefficient for (instantaneous) pore loss follows from the change in the zero-order moment; it may be inferred from the (total) loss of porosity after subtracting the (gradual) loss due to drift toward smaller pores. Estimation of the dispersion coefficient is hampered by our lack of understanding of the behavior of the variance of the PSD. Experimental pore-size data by Laliberte and Brooks (1967) and Shcherbakov et al. (1995) indicate that the variance of static PSDs increases with porosity and mean pore size. Or et al. (2000), therefore, postulated that dispersion and drift coefficients are linearly related for dynamic PSDs because drift presumably depends on mean pore radius and porosity. For lack of experimental information, we related the drift and dispersion coefficients in the same way as for solute transport:

$$\lambda = \frac{D(t)}{|V(t)|} \tag{6}$$

where λ is the dispersivity (μm). Note that the drift coefficient will generally be negative because the pore radius tends to decrease after soil tillage.

The solution of (1) subject to (2) through (4) is obtained with a Laplace transform after eliminating the degradation factor by changing the dependent variable and by using the cumulative drift term as independent variable instead of time. The following solution for the PSD may be obtained (Leij et al., 2002):

$$\begin{aligned} f(r,T) = \exp\left(\int_0^T \frac{M(\tau)}{V(\tau)}\,\mathrm{d}\tau\right) \int_0^\infty f_0(\xi) \\ \times \left\{ \frac{1}{\sqrt{4\pi\lambda T}} \left[\exp\left(-\frac{(r-\xi+T)^2}{4\lambda T}\right) \right.\right. \\ \left.\left. + \exp\left(-\frac{r}{\lambda} - \frac{(r+\xi-T)^2}{4\lambda T}\right)\right] \right. \\ \left. + \frac{1}{2\lambda} \exp\left(-\frac{r}{\lambda}\right) \operatorname{erfc}\left(\frac{r+\xi-T}{\sqrt{4\lambda T}}\right) \right\} \mathrm{d}\xi \end{aligned} \tag{7}$$

where τ and ξ are dummy integration variables while the cumulative drift term, T (μm), is defined by (e.g., Barry and Sposito, 1989)

$$T(t) = -\int_0^t V(\tau)\,\mathrm{d}\tau \tag{8}$$

Eq. (7) provides a general solution for which the time-dependent coefficients V, D, and M that capture the dynamics of pore-size evolution still need to be specified. If experimental observations for the PSD are available, the coefficients may be estimated from explicit expressions for changes in mean, variance, and porosity; this is the approach followed in population dynamics (Hara, 1984). Parametric forms may also be used for the coefficients in the analytical solution, which can be optimized to the experimental information for parameter determination. Alternatively, transport coefficients can be described with a mechanistic model such as the coalescence model by

Ghezzehei and Or (2000). In this case, model parameters may be obtained from independent measurements.

Moments are defined by integrating the PSD with respect to pore-size:

$$m_n(T) = \int_0^\infty r^n f(r,T)\,\mathrm{d}r, \quad n = 0,1,2,\ldots \tag{9}$$

Moments can be quite useful to quantify and analyze experimental and theoretical results. Numerical values for moments require data for the distribution $f(r)$, which may be established experimentally or theoretically. Algebraic expressions for moments can also be obtained according to (9) by using an analytical solution for the PSD. Normalized moments are obtained through division by the zero-order moment (i.e., $M_n = m_n/m_0$). It is customary to characterize the mean with the first-order normalized moment while the variance is given by the second-centralized moment $\mu_2 = M_2 - M_1^2$. Expressions for moments of the PSD according to Eq. (7) are given in Leij et al. (2002).

3. Applications

3.1. Logistic equation

The drift term may be described by the following mathematically convenient and popular expression (cf. Thornley, 1990):

$$V(t) = \frac{\mathrm{d}}{\mathrm{d}t}\langle r\rangle = a\left(1 - \frac{\langle r\rangle}{b}\right)\langle r\rangle,$$

$$\text{where} \quad \langle r\rangle = \frac{b\langle r_0\rangle}{\langle r_0\rangle + (b - \langle r_0\rangle)\exp(-at)} \tag{10}$$

where $\langle r\rangle$ is the mean pore-size (μm) and a and b the empirical coefficients that characterize the temporal and the absolute value of the drift term. Note that $T = \langle r\rangle - \langle r_0\rangle$. We assume that there is no degradation. Fig. 1 shows the predicted PSD after 30 and 120 days as well as the initial distribution. For the solution we assumed that there was no decay, a constant dispersivity $\lambda = 1\,\mu\mathrm{m}$ (Fig. 1a) or $\lambda = 0.1\,\mu\mathrm{m}$ (Fig. 1b) and a time-dependent drift term $V(t)$ given by Eq. (10) with $a = 0.01\,\mathrm{per\,day}$, $b = 5\,\mu\mathrm{m}$, and $\langle r_0\rangle = 7.26\,\mu\mathrm{m}$. The behavior of the velocity is shown in the inset of Fig. 1a. Characteristic moments for mass balance (m_0), mean (M_1) and variance (μ_2) are given for both dispersivities. The PSD shifts toward smaller pores. Fig. 1 illustrates that the drift of probability from larger to smaller pores gradually diminishes with time as quantified by the values for M_1 or $\langle r\rangle$ at the three times.

Fig. 1a shows that dispersion causes the maximum probability to decrease for larger times and to occur at a lower pore-size, i.e., $f(r = 6.8\,\mu\mathrm{m},\ t = 0\,\mathrm{day}) = 0.062\ \mu\mathrm{m}^{-1}$, $f(6.3, 30) = 0.051\,\mu\mathrm{m}^{-1}$, and $f(5.4, 120) = 0.042\,\mu\mathrm{m}^{-1}$. Because zero probability flow is stipulated at $r = 0$, probability is "reflected" for larger times ($t = 120\,\mathrm{days}$). The value for m_0 suggests that probability was preserved. Fig. 1b demonstrates that for a lower dispersivity the shape of the PSDs will remain closer to the initial distribution with maxima $f(6.1, 30) = 0.061\,\mu\mathrm{m}^{-1}$, and $f(5.1, 120) = 0.059\,\mu\mathrm{m}^{-1}$.

3.2. Static retention data for different tillage regimes

Detailed measurements on the evolution of the PSD over time are scarce. However, several studies have been conducted on the effect of tillage on soil hydraulic properties (Ehlers, 1976, 1977; Mapa et al., 1986; Ball and O'Sullivan, 1987; Richard et al., 2001). Water retention is of particular interest. Ahuja et al. (1998) parameterized water retention data with the equation by Brooks and Corey (1964). They were able to obtain adequate predictions of the water retention curves for tilled soils from data for corresponding untilled soils using scaling procedures. We are interested in water retention data because they can be readily converted into a PSD, provided that we can conceptualize soil pores as cylindrical capillaries with soil matric potential given by the Laplace–Young equation. There are, of course, more accurate ways to characterize the PSD such as with mercury intrusion, surface adsorption, and optical methods (Scheidegger, 1972). We will use retention data for different tillage treatments from Germany and Canada as surrogate data to illustrate the application of our model for the evolution of the PSD. In the German example, we attempt to describe the evolution of PSD from a soil with tillage to a similar one with no or minimum tillage. In the Canadian example, we consider the evolution from the PSD due to trafficking.

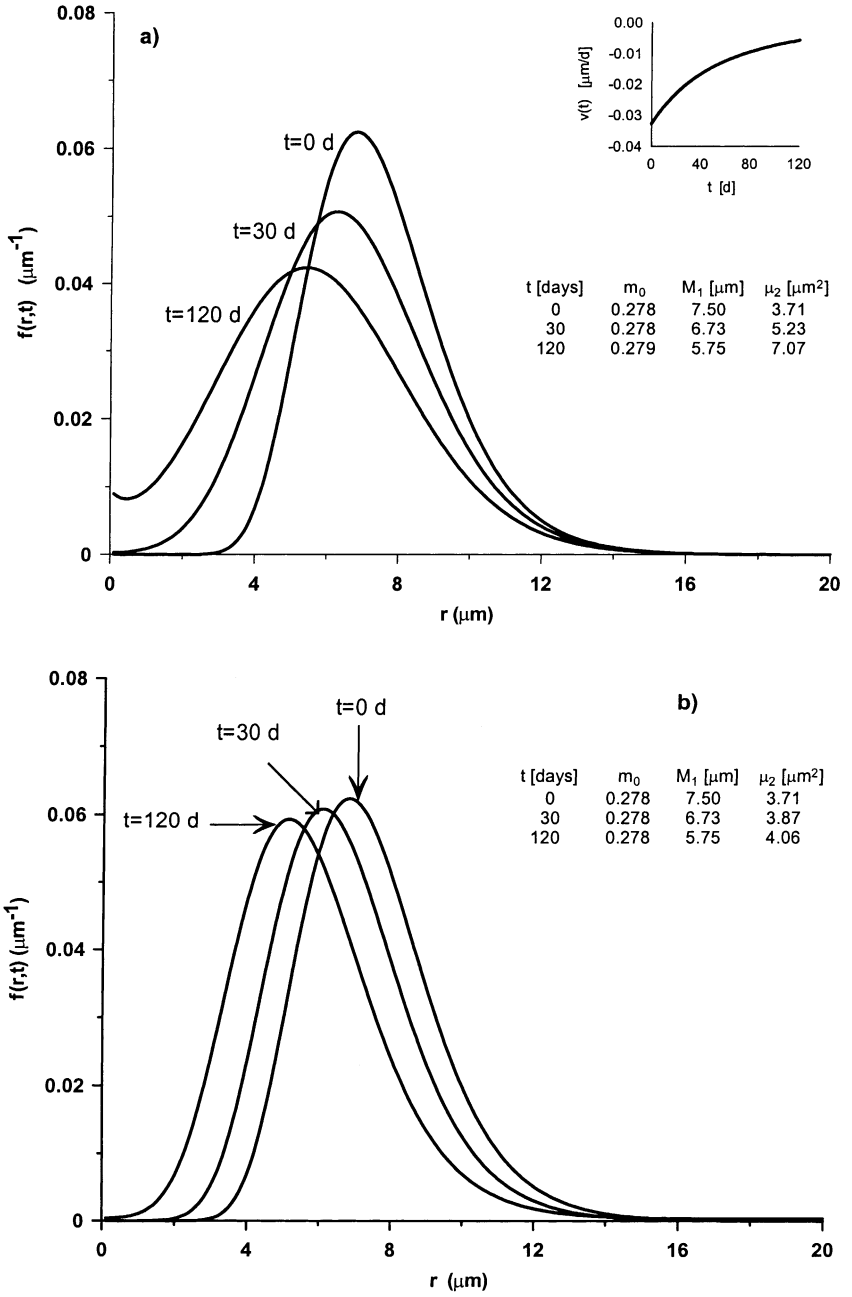

Fig. 1. Evolution of PSD over time according to (7) with no decay, a time-dependent drift term $V(t)$ given by Eq. (10) with $a = 0.01$ per day, $b = 5\,\mu m$, $\langle r_0 \rangle = 7.26\,\mu m$ (shown in inset), and a constant dispersivity: (a) $\lambda = 1\,\mu m$ and (b) $\lambda = 0.1\,\mu m$.

3.2.1. Teiwes (1988) data set—Germany

From the database of unsaturated hydraulic properties UNSODA by Leij et al. (1996), we selected two examples involving samples taken from the top 30 cm of a silt loam as reported by Teiwes (1988). In the first case, retention curves were reported for plots with no tillage for 18 years (code 1340) and with annual moldboard plowing (code 1350) near Goettingen in

Germany. The second case involves similar retention curves with reduced tillage (preparation of a 10 cm seedbed with a rotary harrow) and moldboard plowing (codes 2000 and 2010, respectively). The retention data were obtained with a pressure plate apparatus in the laboratory on six replicate undisturbed core samples. The samples were taken in May 1984, whereas the plowing typically took place in mid-October (W. Ehlers, personal communication). We parameterized the reported data with the expression (cf. Kosugi, 1994):

$$S_e = \frac{\theta - \theta_r}{\theta_s - \theta_r} = \frac{1}{2}\,\mathrm{erfc}\left(\frac{\ln(\psi/\psi_0) - \sigma^2}{\sqrt{2}\sigma}\right) \tag{11}$$

where ψ is the soil matric potential, σ a model parameter (cf. Eq. (5)), and S_e denotes the effective saturation. The inflection point of the water retention curve is determined by ψ_0, which also represents the mode of the soil water capacity function. The top part of Table 1 shows database codes, bulk density (ρ_b), type of tillage, and data regarding the optimization of the retention data such as parameter values, the mean square of residuals for error (MSE) and the coefficient of determination (r^2). Fig. 2a and b shows the retention data and the optimized curves. Eq. (11) provides a satisfactory description of the experimental data. These silt loams have a wide range of particle sizes and the retention curves do not exhibit a distinct air-entry point. Consequently, the values for ψ_0 are relatively low while there is a considerable spread (i.e., high σ).

To calculate the PSD, we used the equality $\psi_m = \psi_0 \exp(\sigma^2)$. The water content corresponding to the median ψ_m is given by $\frac{1}{2}(\theta_s + \theta_r)$. We determined the PSD by first differentiating $\theta(\psi)$ in terms of ψ_m rather than ψ_0, to obtain the water capacity function, $C(\psi) = -\mathrm{d}\theta(\psi)/\mathrm{d}\psi$. We then applied the chain rule and changed the independent variable with $r = A/\psi$, with A as a proportionality constant determined by the variables in the Laplace–Young equation, to obtain

$$f(r) = \frac{\mathrm{d}\theta(\psi)}{\mathrm{d}r} = -C(\psi)\frac{\mathrm{d}\psi(r)}{\mathrm{d}r} \tag{12}$$

The PSD can now be written in the familiar form (cf. Eq. (5)):

$$f(r) = \frac{\theta_s - \theta_r}{r\sigma\sqrt{2\pi}} \exp\left(-\frac{[\ln(r/r_m)]^2}{2\sigma^2}\right), \quad 0 < r < \infty \tag{13}$$

The median pore radius, r_m (μm), which was determined from ψ_m (hPa) assuming that $A = -1490$ hPa μm (Brutsaert, 1966), is shown in the second column of the bottom part of Table 1. Moments of this distribution readily yield the definitions for mean and variance (Aitchison and Brown, 1963):

$$M_1 = \langle r \rangle = r_m \exp\left(\frac{\sigma^2}{2}\right) \tag{14}$$

$$\mu_2 = r_m^2 \exp(\sigma^2)[\exp(\sigma^2) - 1] \tag{15}$$

In our case, the values for σ^2 obtained from optimization of the retention data are relatively large and imprecise. We, therefore, determined m_0, M_1 and μ_2

Table 1
Retention and PSD parameters for the simulation of the PSD after tillage based upon retention data by Teiwes (1988)

Code	Tillage	ρ_b (g/cm^3)	θ_s	θ_r	ψ_0 (hPa)	σ	MSE × 10^4	r^2
General and retention data								
1340	Zero tillage	1.52	0.392	0.097	2.99	2.33	0.13	0.999
1350	Moldboard	1.36	0.469	0.104	1.37	2.27	1.00	0.994
2000	Reduced tillage	1.62	0.367	0.128	3.92	2.44	0.28	0.996
2010	Moldboard	1.45	0.394	0.142	0.437	2.60	1.14	0.985
	r_m (μm)	m_0	$M_1 = \langle r \rangle$ (μm)	$\mu_2 \times 10^{-3}$ (μm^2)	T (μm)	λ (μm)	MSE × 10^5	r^2
PSD data								
1340	2.15	0.292	20.4	4.82				
1350	6.36	0.360	40.9	11.0	20.5	1.3	1.41	0.891
2000	0.997	0.235	13.0	2.87				
2010	3.97	0.247	37.9	11.2	24.9	0.96	2.04	0.850

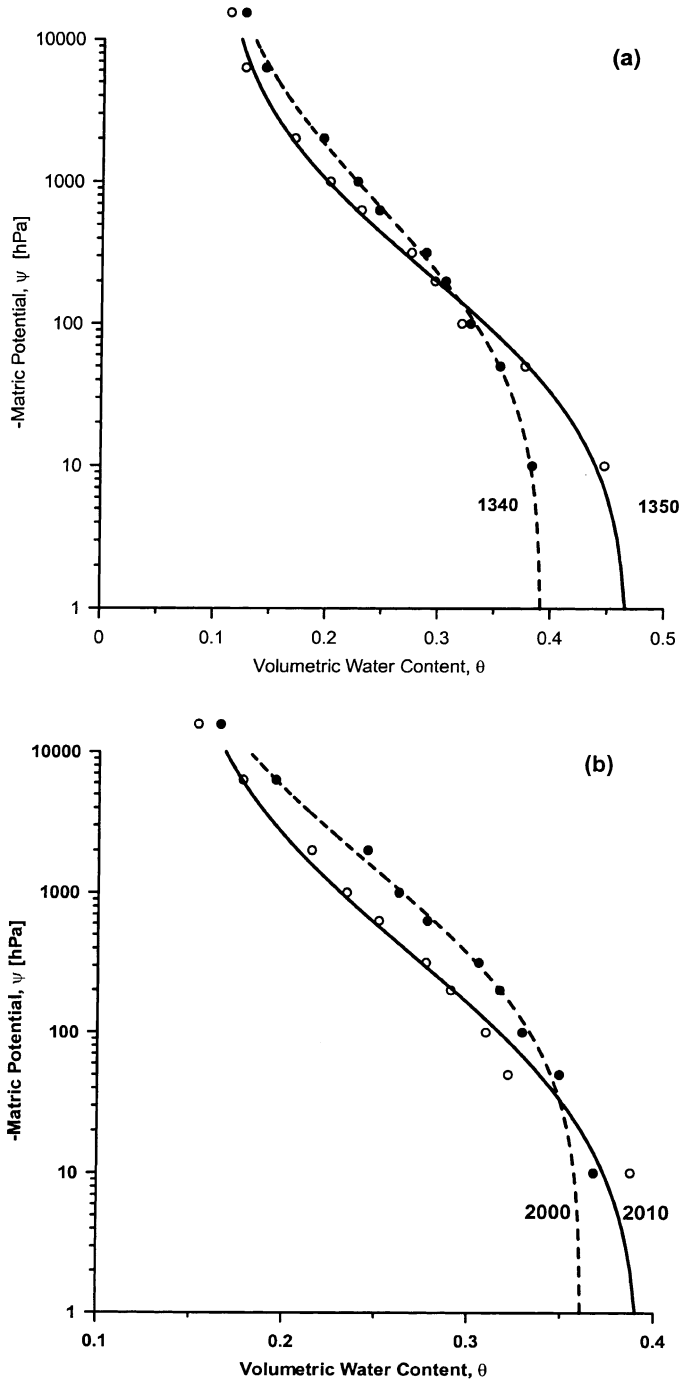

Fig. 2. Optimized curves and retention data according to Teiwes (1988): (a) codes 1340 (zero tillage) and 1350 and (b) codes 2000 (reduced tillage) and 2010.

from moments of the actual PSD computed according to Eq. (5), the resulting values can be found in Table 1.

We postulate that the tilled soil (codes 1350 and 2010) represent the initial condition for the PSD from which evolution occurs to a final state, which is presumably given by the PSD for zero or minimum tillage. Two potential weaknesses in this approach are that tillage treatment cannot readily be converted to time as an independent variable, while the "initial" and "final" retention curves are determined on different samples. Our definition for time according to (8) obviates the first concern if we define the drift term, $V(t)$, as the derivative of the mean pore-size, $\langle r \rangle$, with regular time:

$$T = \langle r(t) \rangle - \langle r(0) \rangle \tag{16}$$

Table 1 shows the resulting values for T. To mitigate the problem of sample difference, we used the final porosity as initial distribution in the solution. The PSD curves for codes 1340 and 2000 were predicted by Eq. (7) using r_m and σ for codes 1350 and 2010 and ϕ_0 for codes 1340 and 2000 in the initial PSD given by Eq. (5). For lack of a better approach, we estimated the dispersivity, λ, with the Levenberg–Marquardt method by fitting Eq. (7) to "observed" PSD-data generated according to Eq. (5). Finally, we assumed that there is no degradation. Table 1 reports the optimization results for λ. We consider the fit reasonable in view of the many assumptions and the fact that only one parameter is optimized.

Fig. 3a and b shows the PSDs for the two examples. The "initial" PSDs of tilled soils 1350 and 2010 are given as dashed lines. It should be noted that these PSDs behave more according to an inverse power law than for a lognormal distribution due to the low r_m and the high σ. The predicted PSDs for the "final" state are shown as solid lines in Fig. 3. Data points depict $f(r)$-values corresponding to the measured retention data. The predictions show a decrease in probability for $r > 2\,\mu m$ while smaller pores become more prevalent for untilled soils. This is in general agreement with the data points. The prediction becomes less accurate for smaller pore radii. This may be because the distribution is not truly lognormal, the analytical solution is less accurate near $r = 0\,\mu m$, and the model is more appropriate for larger inter-aggregate pores. Finally, the same independently determined drift coefficient was used over the entire range of pore radii. Optimizing the drift coefficient or using a formulation that includes pore radius as independent variable may lead to a better prediction. Leij et al. (2002) are investigating a potentially more realistic scenario where the drift coefficient is related to pore radius.

3.2.2. Startsev and McNabb (2001) data set—Canada

Recently, Startsev and McNabb (2001) reported on the effect of skidder traffic on the water retention and water capacity of boreal forest soils of medium texture. Grapple skidders are employed for harvesting and silvicultural operations in forests. Soil samples were taken at 5 and 10 cm depths at 14 study sites subjected to 0, 3, 7, and 12 cycles (constituting an empty and a loaded pass) by different types of skidders, typically with 1.1 m wide tires. The water retention of soil core samples was measured with Tempe pressure cells ($\psi = 20, 50, 100$, and 300 hPa) and a pressure plate extractor ($\psi = 1000$ and 15,000 hPa). The retention data were described by the four-parameter equation of van Genuchten (1980):

$$S_e = \frac{\theta - \theta_r}{\theta_s - \theta_r} = [1 + (\alpha\psi)^n]^{-m}, \quad m = 1 - 1/n \tag{17}$$

We converted the parameter set $\{\theta_s, \theta_r, \alpha, n\}$ into the parameter set for Eq. (11) using the relationships (cf. Kosugi, 1996):

$$\psi_0 = \frac{m^{1-m}}{\alpha} \tag{18}$$

$$\sigma^2 = (1 - m) \ln\left[\frac{2^{1/m} - 1}{m}\right] \tag{19}$$

Table 2 shows the values of the hydraulic parameters for the parametric models by van Genuchten and Kosugi, which are averaged over the eight sites where skidder traffic resulted in significant compaction. The median was, again, computed from $r_m = 1490/\psi_m$, where $\psi_m = \psi_0 \exp(\sigma^2)$. The mean ($\langle r \rangle$) was now calculated according to Eq. (15) rather than from moment analysis. Because the median and mean pore radii did not further decrease for 12 skidder cycles, we omitted this treatment from further analysis.

Fig. 4 shows the retention curves for the three treatments as described by the parameters of the Kosugi model. These curves closely resemble those in Fig. 1 of Startsev and McNabb (2001) according to

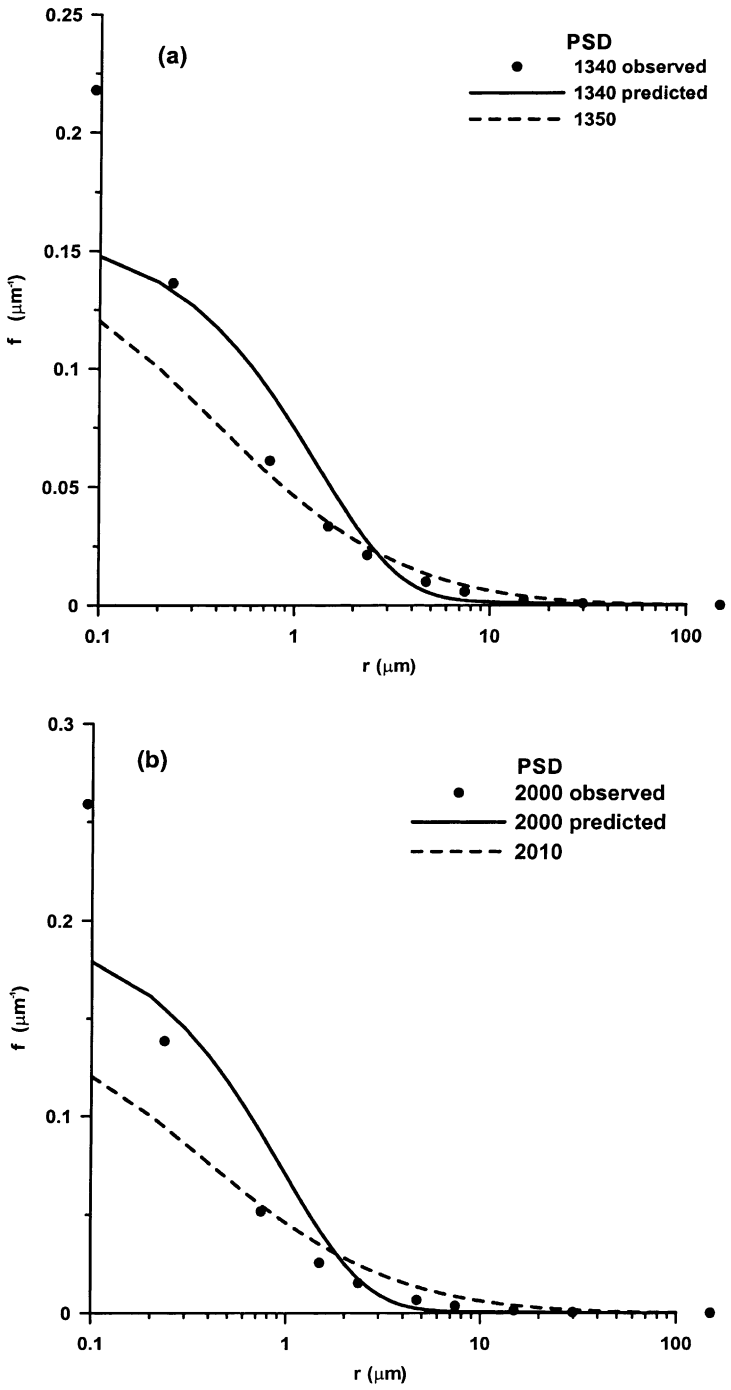

Fig. 3. PSDs according to either Eq. (13), as inferred from water retention data, or Eq. (7) and data in Table 1: (a) initial and observed PSD from retention data for codes 1350 and 1340, and predicted PSD for code 1340 and (b) initial and observed PSD from retention data for codes 2010 and 2000, and predicted PSD for code 2000.

Table 2
Retention and PSD parameters for the simulation of the PSD after 0, 3, and 7 cycles of skidder traffic based upon retention data by Startsev and McNabb (2001)

Number of skidding cycles	θ_s	θ_r	α (hPa^{-1})	n	ψ_0 (hPa)	σ
Retention data						
0	0.55	0.24	0.012	1.94	57.4	0.984
3	0.52	0.27	0.008	1.93	85.7	0.991
7	0.48	0.25	0.006	2.33	131	0.781
	r_m (μm)	$\langle r \rangle$ (μm)	T (μm)	λ (μm)	MSE × 10^5	r^2
PSD data						
0	9.87	16.0				
3	6.51	10.6	5.37	8.3	0.75	0.837
7	6.18	8.38	7.63	9.5	1.56	0.698

the van Genuchten model. The behavior of the retention curves suggests that there is a shift from larger to smaller pores for increased skidder traffic. This is precisely the scenario that we attempt to depict with our mathematical model for pore-size evolution although compaction by skidders represents a different application than tillage of agricultural soils.

Fig. 5a and b shows the relevant PSDs for 3 and 7 cycles, respectively. The dashed lines again represent the ''initial'' condition of no compaction (i.e., 0 cycles)

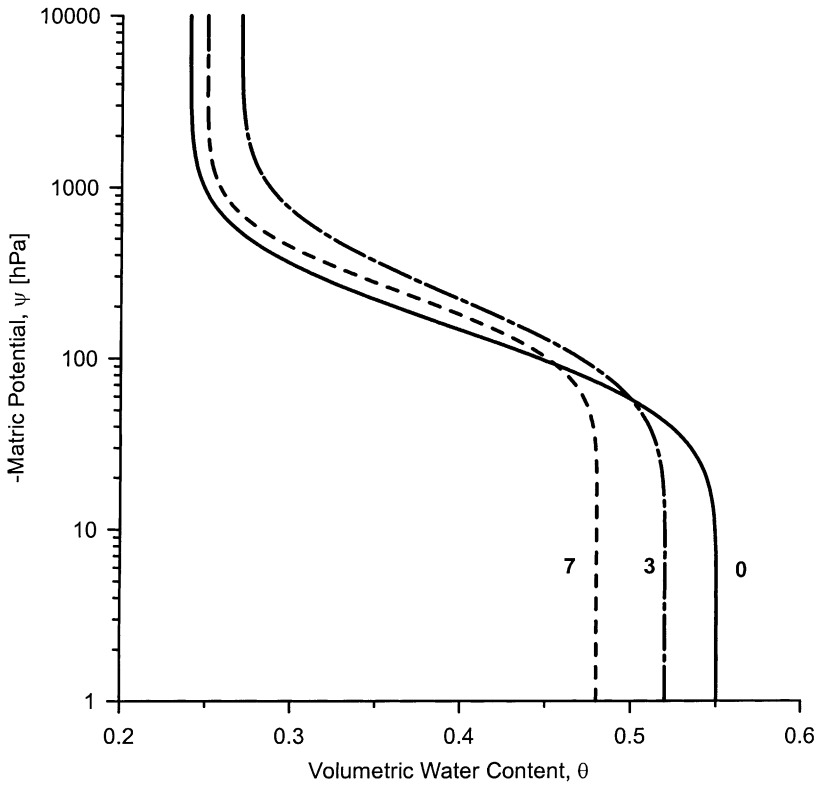

Fig. 4. Water retention curves for 0, 3, and 7 skidder cycles according to Startsev and McNabb (2001).

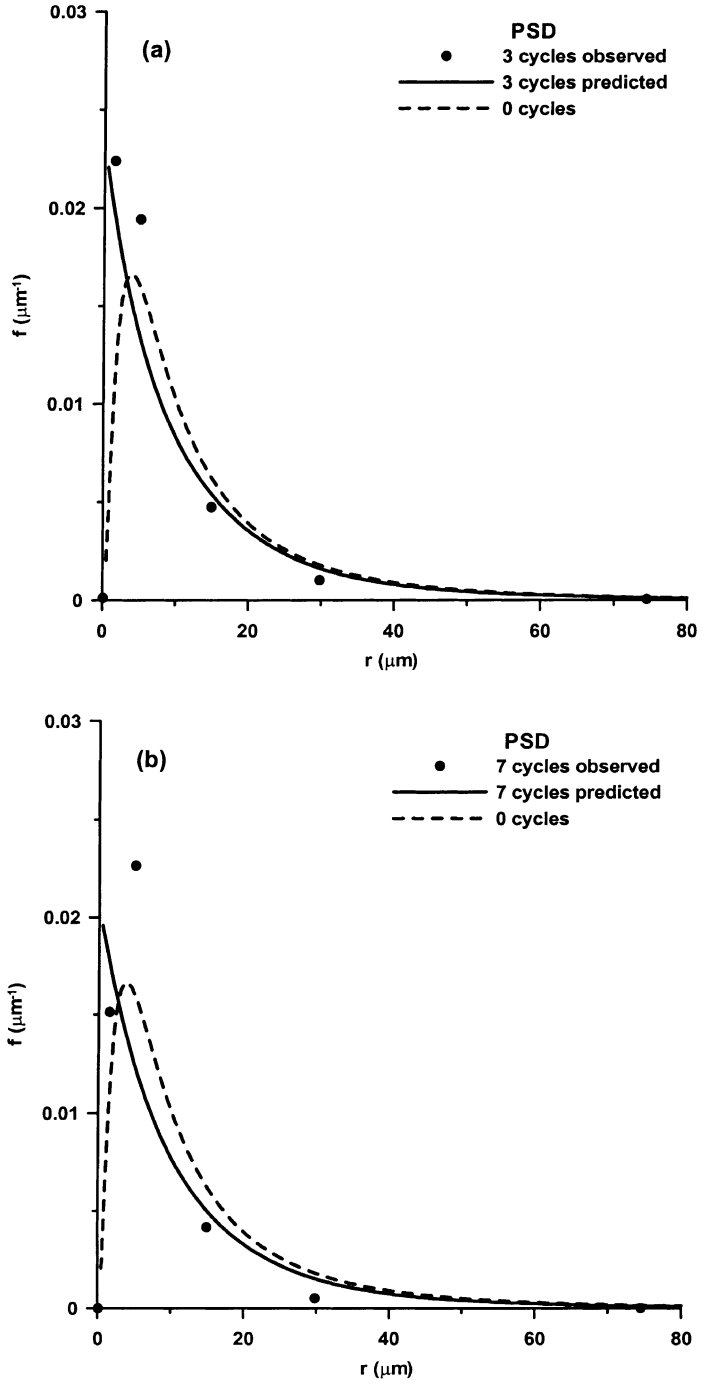

Fig. 5. PSDs according to either Eq. (13), as inferred from water retention data, or Eq. (7) and data in Table 2: (a) initial and observed PSD from retention data for 0 and 3 skidder cycles, and predicted PSD for 3 skidder cycles, and (b) initial and observed PSD from retention data for 0 and 7 skidder cycles, and predicted PSD for 7 skidder cycles.

as quantified by Eq. (5). The PSDs for this example more closely resemble lognormal functions than for the previous example involving German soils. Predictions of the PSD after 3 and 7 skidding cycles were made using the difference in mean pore radius, T, as a drift term with the initial distribution based upon r_m and σ for 0 cycles and ϕ_0 for 3 or 7 cycles. These are depicted as solid lines. The dispersivity was obtained by optimizing the analytical solution given by Eq. (7) to results for the "final" (compacted) PSD using r_m, σ and ϕ_0 for 3 or 7 cycles. Once again, degradation was not included in the model. Data points represent $f(r)$-values for matric potentials at which the retention was measured. The predicted PSDs confirm that compaction leads to a reduction in mean pore radius with an increased probability for smaller pores ($r < 5\,\mu m$). The prediction is poorer for 7 than for 3 cycles, presumably because the use of a single value for T is less accurate over the wider range of 7 cycles. A parametric model for the drift term based upon more detailed measurements of the PSD may lead to more realistic predictions.

3.3. Dynamic hydraulic properties for wetting–drying cycles

In the following application, we will estimate the coefficients of the FPE using the physically based coalescence model by Ghezzehei and Or (2000) to simulate the seasonal evolution of the PSD and associated hydraulic functions using measurements by Mapa (1984). Our purpose is to demonstrate the potential of the pore-size evolution model by comparing model predictions and field-scale observations. We start by providing some brief background information on the experiment. We will then formulate pertinent information about the coalescence model followed by data pertaining to the coalescence model (matric potential, structural porosity, and drift term) and simulation results for the PSD. Finally, we compare observed and predicted hydraulic properties.

3.3.1. Field data

Mapa (1984) measured soil structural and hydraulic properties during five irrigation cycles on a Molokai silty clay loam in Oahu, Hawaii. The soil was tilled to a depth of 40 cm while the water content was approximately 0.2 m^3/m^3 prior to the experiments. One set of hydraulic properties was measured immediately after tillage. The plots were then subjected to five irrigation cycles using a drip-system at intervals of 7–10 days. The plots were covered with a plastic roof at 30 cm above the ground to prevent raindrop impact. The hydraulic properties were measured after each wetting and drying cycle. Porosities and water retention curves were determined in the laboratory on undisturbed soil samples while the hydraulic conductivity was obtained using the simplified drainage flux method. Further details of the experiments can be found in Mapa (1984) and Mapa et al. (1986).

3.3.2. Estimation of FPE coefficients with coalescence model

Ghezzehei and Or (2000) presented a model for the coalescence of soil aggregates based on an energy balance for capillary and rheological processes following earlier work by Or (1996). The model was used by Or et al. (2000) to approximate the FPE coefficients and is also described by Or and Ghezzehei in this issue. For mathematical simplicity, Or et al. (2000) considered a unit-cell model, formed by cubic packing of spherical aggregates (Fig. 4c in Or and Ghezzehei, 2002), to represent the entire structural (inter-aggregate) pore space. The unit-cell pore radius (R) is equated to the geometric-mean radius (r_m) of the initial PSD. In this example, we use rhombic packing of aggregates instead of cubic arrangement.

The complex void space of the unit-cell is represented by a volume-equivalent spherical pore with radius R. The ratio of the pore volume to the total volume of the unit-cell defines the porosity of the unit-cell (ϕ). The pore radius and porosity of the unit-cell are related to the aggregate radius (a) and the time-dependent inter-aggregate strain (ε) by

$$R(t) = a\left[\frac{3\{2[1-\varepsilon(t)]\}^3}{4\pi} - 1\right]^{1/3} \tag{20}$$

$$\phi(t) = 1 - \frac{4\pi}{3\{2[1-\varepsilon(t)]\}^3} \tag{21}$$

where $\varepsilon(t)$ is defined as the ratio h/a, h being the reduction in distance between aggregate center and plane of contact between two aggregates as a result of coalescence An expression for $\varepsilon(t)$ is given by Eq. (15) of Or and Ghezzehei (2002).

The drift coefficient is again considered equivalent to the rate of change of the mean pore radius. It may be obtained in terms of the coalescence model by differentiating (20):

$$V(t) = \frac{\partial R(t)}{\partial \varepsilon}\frac{\mathrm{d}\varepsilon}{\mathrm{d}t} \tag{22}$$

where we make again the assumption that all pore radii drift at the same rate, which circumvents the physically and mathematically more challenging task of formulating a drift term that depends on pore radius. The dispersion coefficient is obtained according to Eq. (6). The degradation coefficient, M, was estimated from the reduction in total porosity. This reduction is due to a gradual decrease in pore radius by viscous deformation of soil aggregates, i.e., the drift process, and instantaneous closure of pores, i.e., the degradation process. The degradation coefficient can be formally defined as the derivative of the zero-order moment given by Eq. (9). For the estimation of M from porosity data, we assume that the complete pore closure is linearly related to the gradual decrease in pore radius (porosity) by

$$M(t) \equiv \frac{\partial m_0}{\partial t} \approx \frac{\Delta\phi_\mathrm{c}}{\Delta t} = \delta\frac{\partial\phi(t)}{\partial h}\frac{\mathrm{d}h}{\mathrm{d}t} \tag{23}$$

where m_0 is the zero-order moment, $\Delta\phi_\mathrm{c}$ denotes porosity loss due to closure, δ a constant denoting the fraction of porosity loss due to complete pore closure, and h the loss in aggregate radius due to coalescence.

3.3.3. Simulations

The soil pore system is partitioned into textural and structural components (cf. Nimmo, 1997). The latter being far more susceptible to changes due to wetting and drying processes. We illustrate the use of the FPE to describe the evolution of a bimodal PSD by assuming an evolving inter-aggregate porosity (structural) and a stationary intra-aggregate porosity (textural). The initial inter-aggregate pore space is described by the lognormal PSD given by Eq. (5) with a median or geometric mean pore radius ($r_0 = 24\,\mu\mathrm{m}$) equal to the initial pore radius of the unit-cell, a prescribed log-transformed variance ($\sigma^2 = 0.8$) and a porosity fraction ($\phi_1 = 0.22$). The intra-aggregate porosity is described by a similar lognormal distribution with prescribed parameters ($r_0 = 4\,\mu\mathrm{m}$, $\sigma^2 = 0.5$, $\phi_2 = 0.348$). These parameters were selected such that the initial soil water characteristic curve matches the experimental measurements of Mapa (1984).

The aggregate bed is subjected to five wetting and drying cycles. Aggregate coalescence will occur due to the flow of soil material toward inter-aggregate contacts, which is described by the Bingham model with plastic viscosity η_p (Pa s) and yield stress τ_y (Pa). Since these rheological variables are not available for the Molokai silty clay loam, we used measurements for a Millville silt loam (cf. Or and Ghezzehei, 2002). The primary driving force for coalescence is the soil water potential. If the soil is very wet, the capillary forces may be insufficient to exceed the soil strength (i.e., the yield stress) or there may not even be an air–water interface to provide energy for the coalescence. On the other hand, coalescence may terminate for dry soils when the yield stress increases while the driving force fueled by capillarity tends to decrease for smaller aggregates. A detailed explanation of the interplay between soil rheological properties and capillary forces during drying is given by Ghezzehei and Or (2000). The simulated matric potential during the initial periods of each drying phase is shown in Fig. 6a, there is a 7- to 10-day interval between each wetting–drying cycle. The corresponding evolution of unit-cell porosity according to (21) (representing structural porosity) is depicted in Fig. 6b. Note that, the reduction in porosity is larger for the third than for the second drying cycle because there is less opportunity for coalescence during the second cycle with its rapidly decreasing matric potential. The FPE coefficients were calculated according to Eq. (22), using Eq. (6) with $\lambda = 0.05\,\mu\mathrm{m}$, and (23) with $\delta = 0.7$. The drift coefficient is shown in Fig. 6c as a function of time. The above matric potential functions were selected to match predicted and measured porosities at the end of each wetting–drying cycle while values for the FPE coefficients were selected to generate a PSD according to the observed retention data.

The evolution of the PSD is a reflection of the change in soil matric potential simulated numerically using an explicit finite difference scheme. The complicated behavior of the drift coefficient with time makes use of the analytical solution equation (23) slightly less convenient. Fig. 7a shows the inter-aggregate PSD

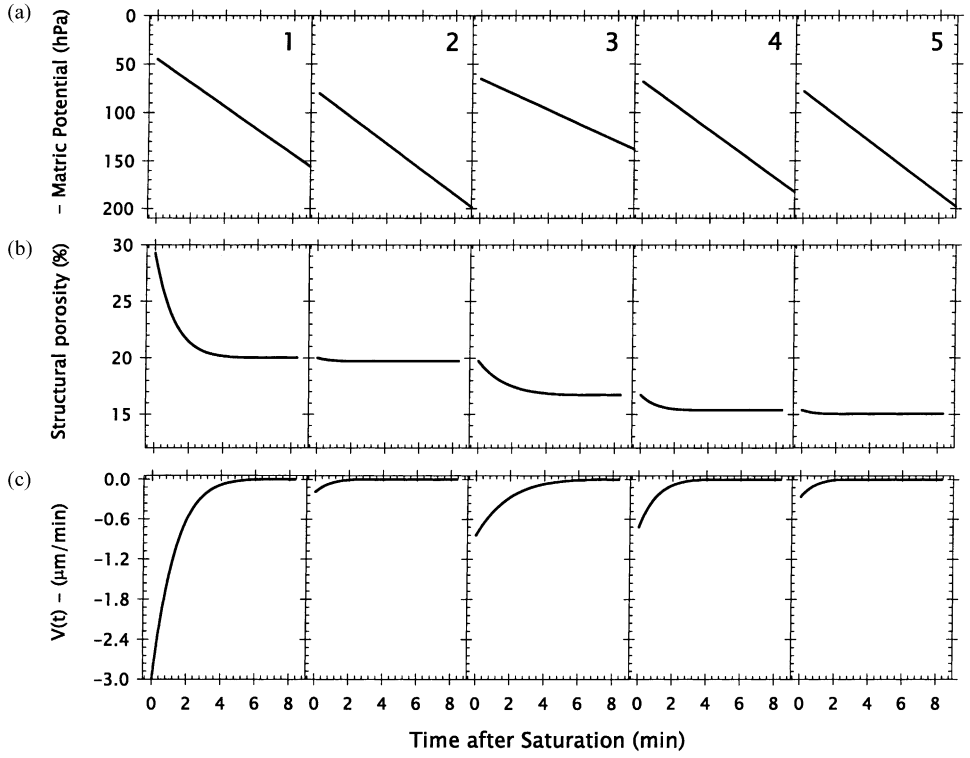

Fig. 6. Temporal behavior of matric potential, inter-aggregate porosity, and drift coefficient during initial drying stage of five subsequent cycles.

at the start of the experiment as well as at the end of the first and fifth drying cycles. All changes in the PSD are attributed to evolution of the structural pore system, while the textural PSD is assumed constant. For the "structural" pore space, the median pore radius (r_m) diminishes with time, while the variance of the PSD increases (indicated by increased spread of structural PSD in Fig. 7a). The frequency of the

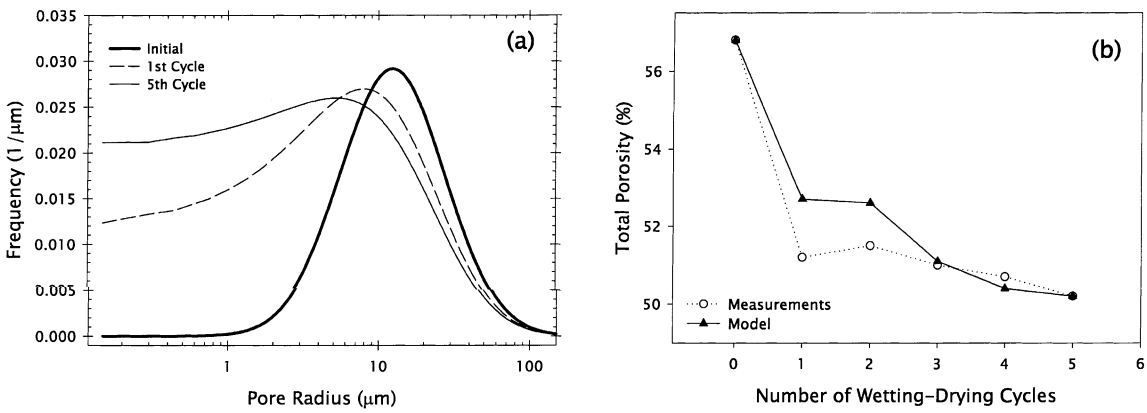

Fig. 7. Evolution of soil PSD during wetting and drying: (a) initial PSD and the PSD at the end of the first and fifth period of drying, and (b) measured and predicted total porosity as a function of the number of wetting–drying cycles.

smallest structural pores increases with each drying cycle as inter-aggregate pores become smaller. The evolution of the total porosity, as calculated from the change in expected pore volume, is shown in Fig. 7b. The simulated trend in porosity corresponds favorably to measured values.

3.3.4. Estimation of soil hydraulic functions

The evolution of the PSD is a reflection of the soil water retention curve, which allowed us earlier to infer the PSD from retention measurements. Conversely, the water retention curve may be obtained from integration of the PSD (cf. Eq. (12)):

$$\theta(\psi) = \int_{-\infty}^{\psi} C(\psi)\,\mathrm{d}\psi + \theta_\mathrm{r} \quad \text{with} \quad C(\psi) = -\frac{\mathrm{d}\theta}{\mathrm{d}\psi} \tag{24}$$

where θ_r is again the residual water content. The water retention curve according to Eq. (24) is shown in Fig. 8. The modeled retention curves closely describe the observations.

A potentially important application of the stochastic pore-size evolution model is the prediction of temporal changes in the saturated and unsaturated hydraulic conductivity, K_s and $K(\phi)$, respectively. For illustrative purposes, the Kozeny–Carman relationships are used to estimate changes in the saturated hydraulic conductivity from changes in total porosity (Berryman and Blair, 1987).

$$K_\mathrm{s}(t) = \frac{\phi(t)^2}{cFA_\mathrm{s}[1-\phi(t)]^2}\frac{\rho g}{\eta} \tag{25}$$

where $K_\mathrm{s}(t)$ is saturated hydraulic conductivity at time t, c a weak function of the pore geometry, A_s the specific surface area of the porous media, F the electrical formation factor, ρ and η the density and viscosity water, and g the gravitational acceleration. The formation factor is related to porosity and pore geometry by (Revill and Cathles, 1999)

$$F = \phi(t)^{-m} \tag{26}$$

where m is the so-called cementation exponent, which varies with the pore geometry inside a range 1–4 (Sen et al., 1981). When the estimated saturated hydraulic conductivity ($K_\mathrm{s}(t)$) is written with respect to the initial saturated conductivity ($K_\mathrm{s}(0)$), the Kozeny–Carman equation yields the following expression for the relative saturated conductivity in terms of time-dependent porosity:

$$\frac{K_\mathrm{s}(t)}{K_\mathrm{s}(0)} = \left(\frac{\phi(t)}{\phi(0)}\right)^{2m}\left(\frac{1-\phi(0)}{1-\phi(t)}\right)^2 \tag{27}$$

As the Kozeny–Carman model is based on granular porous media, Eq. (27) was evaluated using the

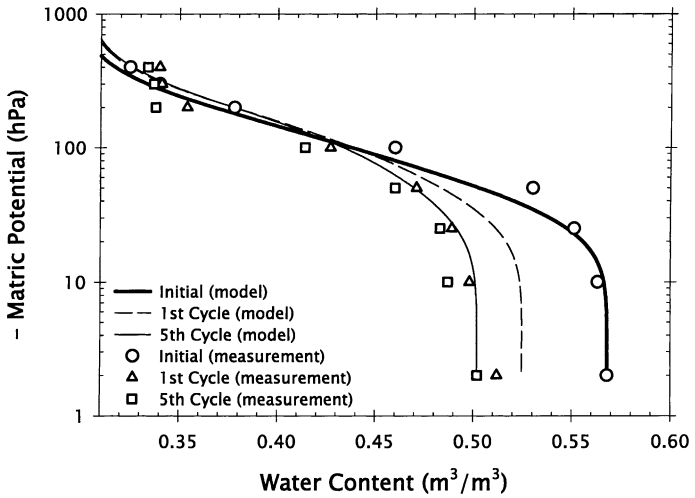

Fig. 8. Evolution of soil water retention during drying–wetting cycles as illustrated by measured and modeled retention data at the start of the experiment and at the end of the first and fifth period of drying.

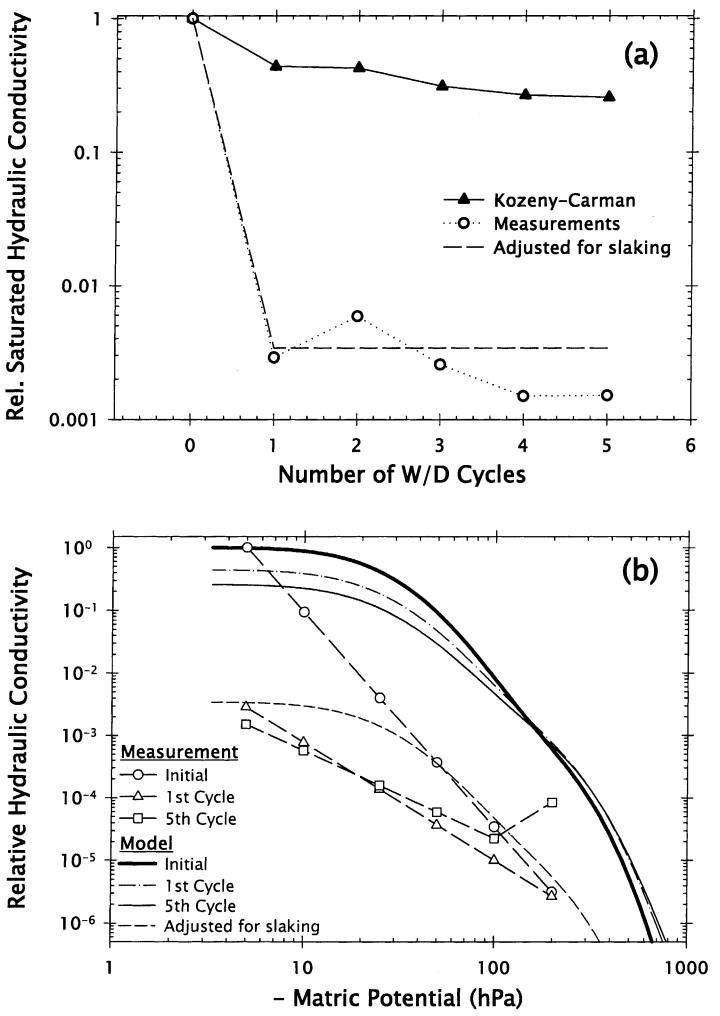

Fig. 9. Evolution of hydraulic conductivity: (a) saturated conductivity as a function of the number of wetting–drying cycles and (b) unsaturated conductivity function at the start of the experiment and at the end of the first and fifth period of drying.

structural porosity. The relative saturated hydraulic conductivity for the wetting–drying example is shown in Fig. 9a. The predictions according to the Kozeny–Carman model could not capture the large reduction in saturated hydraulic conductivity that was observed in the field (circles denote the experimental data). This discrepancy may be due to structural changes (e.g., slaking) near the soil surface (Or, 1996). The coalescence model does not describe such changes in K_s. The predictions of the Kozeny–Carman model were modified by considering that slaking during initial wetting reduced the porosity of surface soils to the value of initial textural porosity (dashed lines in Fig. 9a).

The behavior of the relative unsaturated hydraulic conductivity (K_r) may be predicted from the water retention curve and the saturated conductivity according to Mualem (1976):

$$K_r = \frac{K(t,\psi)}{K_s(0)} = S_e^{1/2}\left\{\frac{\int_0^{S_e} dx/|\psi(x)|}{\int_0^1 dx/|\psi(x)|}\right\}^2 \tag{28}$$

where the relative saturation (S_e) is given by Eq. (11). Fig. 9b shows the relative unsaturated hydraulic conductivity with respect to the initial saturated hydraulic conductivity. The original model provides a poor prediction of the data. If adjusted values for the

saturated conductivity are employed, the predictions improve markedly. The reduction in structural pore space reduces the conductivity more strongly than the retention curve, presumably due to increased tortuosity. These simulations suggest that additional mechanisms for structural change should be added to the current coalescence model to reflect such a reduction.

4. Summary and conclusions

The constant state of change in surface soil layers of agricultural fields presents a challenge to hydraulic characterization and modeling. Key variables affecting soil hydraulic properties are porosity and the PSD. We have proposed a stochastic framework for the evolution of the PSD using the FPE. The model accounts for the dynamics of the mean and variance of the PSD as well the porosity through drift, dispersion, and degradation coefficients. These coefficients can be estimated either from independent measurements or from models. For the first approach we relied on retention data, which were parameterized with the retention model of Kosugi (1994). For the second approach, we relied on a previously developed mechanistic model of soil aggregate coalescence that predicts aggregate strain (Or, 1996; Ghezzehei and Or, 2000). The drift term was estimated from the rate of change of the mean pore radius. The lack of information on the behavior of the instantaneous variance $D(r,t)$ required conjecture that a similar proportionality exists between V and D as for solute transport, although rather limited experimental data seems to support such a ''dispersivity'' for pore-size evolution. The degradation coefficient can be estimated from the reduction in total porosity provided that a distinction can be made between porosity loss due to gradual drift and instantaneous collapse.

An analytical solution to the model for pore-size evolution was presented, which allows the prediction of the PSD with time and pore radius as independent variables. Several applications of the model were explored. The model was first applied to predict the PSD using a generic drift term. Static measurements of soil water retention for tilled and no-tilled treatments served as surrogates for dynamic changes in the same soil sample. These examples illustrated how one would apply the model and provided insights regarding the form of the drift and dispersion coefficients of the FPE. Reasonably accurate prediction of the PSD were possible, the predictions could be enhanced if more accurate inter-aggregate PSDs and formulations for the drift coefficients were available. An additional example was based on the relatively complete data set of Mapa (1984). The parameters for the FPE were derived from the coalescence model of Ghezzehei and Or (2000). This example illustrates the feasibility of the proposed approach in predicting dynamic changes in soil structural and hydraulic properties.

In this paper, we have shown that a stochastic model with physically based coefficients, however simplified, offers promise for capturing the complex dynamics of agricultural soils. The limiting factor is not the theoretical part, but rather the lack of definitive data on soil structural and hydrological dynamics. We hope that this paper provides the impetus for further experimental investigations of the PSD.

Acknowledgements

The partial funding by USDA/NRI through contract 97-00814, by the United States–Israel Binational Agricultural and Research Fund (BARD) through contract 2794-96, by the Army Research Organization through contract 39153-EV, and by the National Science Foundation through subcontract Y542146 (SAHRA, University of Arizona), as well as the partial support of the Utah Agricultural Experimental Station (UAES) are gratefully acknowledged.

References

Ahuja, L.R., Naney, J.W., Green, R.E., Nielsen, D.R., 1984. Macroporosity to characterize variability of hydraulic conductivity and effects of land management. Soil Sci. Soc. Am. J. 48, 670–699.

Ahuja, L.R., Fiedler, F., Dunn, G.H., Benjamin, J.G., Garrison, A., 1998. Changes in soil water retention curves due to tillage and natural reconsolidation. Soil Sci. Soc. Am. J. 62, 1228–1233.

Aitchison, J., Brown, J.A.C., 1963. The Lognormal Distribution. Cambridge University Press, Cambridge.

Ball, B.C., O'Sullivan, M.F., 1987. Cultivation and nitrogen requirements for drilled and broadcast winter barley on a surface water gley (gleysol). Soil Till. Res. 9, 103–122.

Barry, D.A., Sposito, G., 1989. Analytical solution of a convection–dispersion model with time-dependent transport coefficients. Water Resour. Res. 25, 2407–2416.

Berryman, J.G., Blair, S.C., 1987. Kozeny–Carman relations and image processing methods for estimating Darcy's constant. J. Appl. Phys. 62, 2221–2228.

Brooks, R.H., Corey, A.T., 1964. Hydraulic Properties of Porous Media. Hydrology Paper 3. Colorado State University, Ft. Collins, CO.

Brutsaert, W., 1966. Probability laws for pore-size distributions. Soil Sci. 101, 85–92.

Durner, W., 1994. Hydraulic conductivity estimation for soil with heterogeneous pore structure. Water Resour. Res. 30, 211–223.

Ehlers, W., 1976. Rapid determination of unsaturated hydraulic conductivity in tilled and untilled loess soil. Soil Sci. Soc. Am. J. 40 (6), 837–840.

Ehlers, W., 1977. Measurement and calculation of hydraulic conductivity in horizons of tilled and untilled loess-derived soil, Germany. Geoderma 19, 293–306.

Ghezzehei, T.A., Or, D., 2000. Dynamics of soil aggregate coalescence governed by capillary and rheological processes. Water Resour. Res. 36 (2), 367–379.

Gupta, S.C., Larson, W.E., 1982. Modeling soil mechanical behavior during tillage. In: Unger, P.W. (Ed.), Predicting Tillage Effects on Soil Physical Properties and Processes. ASA Special Publications, pp. 151–178.

Hara, T., 1984. A stochastic model and the moment dynamics of the growth and size distribution in plant populations. J. Theoret. Biol. 109, 191–215.

Kosugi, K., 1994. Three-parameter lognormal distribution model for soil water retention. Water Resour. Res. 30, 891–901.

Kosugi, K., 1996. Lognormal distribution model for unsaturated soil hydraulic properties. Water Resour. Res. 30, 891–901.

Laliberte, G.E., Brooks, R.H., 1967. Hydraulic properties of disturbed soil materials affected by porosity. Soil Sci. Soc. Am. Proc. 31, 451–454.

Leij, F.J., Alves, W.J., van Genuchten, M.T., Williams, J.R., 1996. Unsaturated Soil Hydraulic Database. UNSODA 1.0 User's Manual. Report EPA/600/R-96/095. US Environmental Protection Agency, Ada, OK, 103 pp.

Leij, F.J., Ghezzehei, T.A., Or, D., 2002. Analytical solutions to an approximate model for pore-size evolution after tillage. Soil Sci. Soc. Am. J., in press.

Mapa, R.B., 1984. Temporal variability of soil hydraulic properties subsequent to tillage. Ph.D. Dissertation. University of Hawaii, Honolulu (Diss. Abstr., 84-29309).

Mapa, R.B., Green, R.E., Santo, L., 1986. Temporal variability of soil hydraulic properties with wetting and drying subsequent to tillage. Soil Sci. Soc. Am. J. 50, 1133–1138.

Mualem, Y., 1976. A new model for predicting the hydraulic conductivity of unsaturated porous media. Water Resour. Res. 12, 513–522.

Nimmo, J.R., 1997. Modeling structural influences on soil water retention. Soil Sci. Soc. Am. J. 61, 712–719.

Or, D., 1996. Wetting-induced soil structural changes: the theory of liquid phase sintering. Water Resour. Res. 32, 3041–3049.

Or, D., Ghezzehei, T.A., 2002. Modeling post-tillage structural dynamics in aggregated soils: a review. Soil Till. Res. 64, 41–59.

Or, D., Leij, F.J., Snyder, V., Ghezzehei, T.A., 2000. Stochastic model for post-tillage soil pore space evolution. Water Resour. Res. 36 (7), 1641–1652.

Revill, A., Cathles III, L.M., 1999. Permeability of shaly sands. Water Resour. Res. 35, 651–662.

Richard, G., Sillon, J.F., Marloie, O., 2001. Comparison of inverse and direct evaporation methods for estimating soil hydraulic properties under different tillage practices. Soil Sci. Soc. Am. J. 65, 215–224.

Risken, H., 1989. The Fokker–Planck Equation, Springer, Heidelberg.

Scheidegger, A.E., 1972. The Physics of Flow Through Porous Media. The University of Toronto Press, Toronto, Ont.

Sen, P.N., Scala, C., Cohen, M.H., 1981. Self-similar model for sedimentary rocks with application to dielectric constant of fused glass beads. Geophysics 46, 781–795.

Shcherbakov, R.A., Korsunskaya, L.P., Pachepsky, Y.A., 1995. A stochastic model of the soil pore space. Eurasian Soil Sci. 27, 93–100.

Startsev, A.D., McNabb, D.H., 2001. Skidder traffic effects on water retention, pore-size distribution, and van Genuchten parameters of Boreal forest soils. Soil Sci. Soc. Am. J. 65, 224–231.

Teiwes, K., 1988. Einfluß von Bodenbearbeitung und Fahrverkehr auf physikalische Eigenschaften schluffreicher Ackerböden. Ph.D. Dissertation. University of Göttingen, Germany.

Thornley, J.H.M., 1990. A new formulation for the logistic growth equation and its application to leaf area growth. Ann. Bot. London 66, 309–311.

van Genuchten, M.T., 1980. A closed-form equation for predicting the hydraulic conductivity of unsaturated soils. Soil Sci. Soc. Am. J. 44, 892–898.